Mechanism of electrohydrodynamic instability with collinear conductivity gradient and electric field

Surabhi Sharan,[1] Prateek Gupta,[2] and Supreet Singh Bahga[1,*]

[1]*Department of Mechanical Engineering, Indian Institute of Technology Delhi, Hauz Khas, New Delhi 110016, India*

[2]*School of Mechanical Engineering, Purdue University, West Lafayette, Indiana 47907, USA*

(Received 11 November 2016; published 2 February 2017)

We describe the physical mechanism responsible for electrohydrodynamic (EHD) instability of a fluid layer with collinear conductivity gradient and electric field. In particular, we resolve the ambiguity in literature regarding the cause for switching between stationary and oscillatory modes of EHD instability. Using linear stability analysis, we show that a small perturbation in conductivity field perturbs the local electric field and also induces a perturbation charge. The coupling of base-state electric field with the perturbation charge leads to a force which causes overstability. Whereas, the coupling of base-state free charge with perturbation electric field leads to a force which causes EHD instability via a stationary mode. The proposed mechanism correctly explains the existence of stationary and oscillatory modes for varying conductivity gradients and wave number of disturbances, depending upon the relative magnitude of these two forces.

DOI: 10.1103/PhysRevE.95.023103

I. INTRODUCTION

Electric field driven fluid flow and ion-transport are widely used in microfluidic devices for pumping fluids [1,2] and electrophoretic separation and preconcentration of ionic species [3–5]. Electrophoresis techniques, such as field amplified sample stacking [3,6] and isoelectric focusing [4,7] invariably involve diffusive gradients in electrical conductivity that are collinear with externally applied electric field. At high electric fields, which are necessary for electrophoresis techniques, the presence of such conductivity gradients often leads to an undesirable phenomenon of electrohydrodynamic (EHD) instability [8–11]. EHD instability results from the coupling of electric field and fluid motion in the regions with conductivity gradients. The gradients in electric field associated with gradients in conductivity lead to accumulation of free charge in the bulk fluid. This free charge in turn couples with the local electric field to apply a destabilizing electric body force on the fluid [8–11]. In contrast to their detrimental effects on electrophoretic separations, EHD instabilities are desirable in other microfluidic systems for the active mixing of multiple fluid streams with different conductivities [8,12].

EHD instability of a fluid layer with collinear electric field and conductivity gradient was described by Hoburg and Melcher [10] using linear stability analysis over a base state with diffusive conductivity gradient. Their analysis showed that the EHD instability sets in as stationary convection for low wave number disturbances. Whereas, for high wave number disturbances, the system shows overstability which is characterized by oscillatory modes. Although the base state for which stability was analyzed by Hoburg and Melcher [10] developed due to diffusion of ions, they neglected diffusive fluxes in the governing equations. In the absence of molecular diffusion, Hoburg and Melcher [10] predicted the fluid layer to be linearly unstable.

Later, Baygents and Baldessari [11] revisited the problem of Hoburg and Melcher [10] and showed that the diffusion of ions (and conductivity) has a stabilizing effect on the system. However, to obtain the stability criterion, Baygents and Baldessari [11] incorrectly assumed the principle of exchange of stability in their linear stability analysis; that is, instability was assumed in the form of a stationary mode. This assumption was subsequently relaxed by Chang *et al.* [13] who showed that the fluid layer with collinear conductivity gradient and electric field exhibits overstability via oscillatory modes for low conductivity gradients. Whereas, for large conductivity gradients, EHD instability is characterized by stationary and oscillatory modes for small and large wave number disturbances, respectively, which is consistent with earlier predictions of Hoburg and Melcher [10].

Baygents and Baldessari [11] and Chang *et al.* [13] attributed the EHD instability to the destabilizing tendency of a displaced parcel of fluid with low conductivity in a region of high conductivity to move further towards the region with higher conductivity and lower electric field. They referred to this phenomena as dielectrophoretic (DEP) motion, though the migration is due to variation in conductivity and not dielectric permittivity [14]. Note that, DEP usually refers to the phenomenon where a dielectic particle experiences a force when subjected to a non-uniform electric field [14]. Therefore, to avoid confusion in this paper we do not use the term DEP to refer to the destabilizing motion predicted by Baygents and Baldessari [11] and Chang *et al.* [13]. According to Baygents and Baldessari [11] and Chang *et al.* [13] EHD instability sets in when the destabilizing motion is faster than the rate at which molecular diffusion dissipates the conductivity gradient. Therefore, for a given conductivity gradient, EHD instability sets in above a critical value of electric Rayleigh number (Ra_e) [11,13], which is defined as the ratio of time-scales associated with diffusion and electrohydrodynamic flow (also termed as electroviscous flow [10]).

To explain the reason of switching from overstability to stationary EHD instability with an increase in conductivity, Chang *et al.* [13] noted that the electric body force tends to destabilize the system in the form of an oscillatory mode. This description is consistent with the physical mechanism proposed by Hoburg and Melcher [10] for overstability, albeit without diffusive effects. However, at large conductivity gradients, Chang *et al.* [13] noted that diffusive effects become

*bahga@mech.iitd.ac.in

prominent and this results in a transition to stationary mode of instability. The latter observation of Chang *et al.* [13] is questionable. Firstly, the time scale associated with diffusion remains same regardless of the conductivity gradient. Hence, higher base-state conductivity gradient does not lead to faster diffusion of conductivity disturbances. Secondly, the physical mechanism based on diffusive effects does not explain why the EHD instability is dominated by an oscillatory mode for high wave number disturbances, wherein diffusion is prominent. Rather, Hoburg and Melcher [10] predicted this transition of EHD instability from stationary to oscillatory mode with increasing wave number of disturbance even in the absence of diffusion. We note that the physical mechanism for selection between stationary and oscillatory modes of EHD instability was not described by Hoburg and Melcher [10].

In this paper, we resolve this ambiguity regarding the physical mechanism of EHD instability of a fluid layer with collinear conductivity gradient and electric field. For small disturbances at which the system behaves linearly, we show that the electric body force consists of two contributing forces: (i) due to the coupling of base-state electric field with perturbation charge and (ii) due to the coupling of free charge in the base-state with perturbation electric field. In particular, we show that the first force dominates at low base-state conductivity gradients or high disturbance wave numbers, and this force leads to overstability. Whereas, at large base-state conductivity gradients and low disturbance wave numbers, the second force dominates and destabilizes the system in form of a stationary mode.

II. MATHEMATICAL MODELING

We analyze the stability of an initially quiescent layer of a symmetric binary electrolyte solution, shown in Fig. 1, bounded between two boundaries at $z = 0$ and $z = d$ and extending infinitely in the x and y directions. An external electric field is applied along the z-direction. In the base state, the conductivity of the electrolyte increases linearly from $z = 0$ to $z = d$ as

$$\overline{\sigma}(z) = \sigma_a + \frac{\Delta\sigma}{d} z, \tag{1}$$

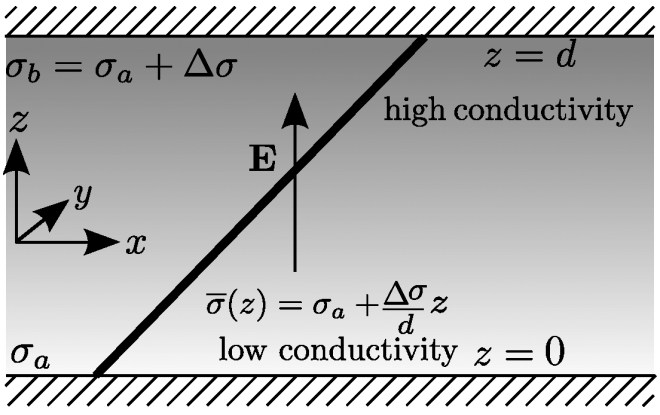

FIG. 1. Schematic illustrating the base state consisting of a quiescent fluid layer between bounding surfaces at $z = 0$ and $z = d$, with collinear conductivity gradient and electric field.

where $\Delta\sigma = \sigma_b - \sigma_a > 0$. Here, σ_b and σ_a denote local conductivity at the upper boundary ($z = d$) and lower boundary ($z = 0$), respectively. The overbar denotes the base-state quantities.

A. Dimensional balance laws

The flow velocity $\mathbf{u}$ in electric field driven, incompressible flow obeys the continuity equation

$$\nabla \cdot \mathbf{u} = 0. \tag{2}$$

The conservation of momentum is described by the Navier-Stokes equations with an additional electric body force term $\rho_f \mathbf{E}$. Assuming that the electrolyte is a linear dielectric with spatially uniform dielectric permittivity ϵ, the electric body force $\rho_f \mathbf{E} = \epsilon(\nabla \cdot \mathbf{E})\mathbf{E}$ due to the Gauss' law ($\epsilon \nabla \cdot \mathbf{E} = \rho_f$). Under these assumptions, the momentum equation simplifies to

$$\rho \frac{\partial \mathbf{u}}{\partial t} + \rho \mathbf{u} \cdot \nabla \mathbf{u} = -\nabla p + \eta \nabla^2 \mathbf{u} + \epsilon(\nabla \cdot \mathbf{E})\mathbf{E}, \tag{3}$$

where ρ, p, and η denote density, pressure, and dynamic viscosity of the liquid.

The transport of cations (+) and anions (−) in a symmetric binary electrolyte solution ($z_+ = -z_- = z$) and $D_+ = D_- = D_0$) due to fluid flow, electric field, and diffusion can be described by

$$\frac{\partial c_\pm}{\partial t} + \mathbf{u} \cdot \nabla c_\pm + \nabla \cdot (\mu_\pm c_\pm \mathbf{E}) = \nabla(D_0 \nabla c_\pm), \tag{4}$$

where c denotes the species concentration, μ the electrophoretic mobility, and D_0 the molecular diffusivity. The species transport equations can be simplified by assuming that the electrolyte solutions is approximately electroneutral $z_+ c_+ \simeq -z_- c_-$ [15–17]. Multiplying the transport equations for cations and anions, Eq. (4), with $z_\pm F$ (F is the Faraday constant) and then adding them yields the equation for continuity of current (Ohm's law),

$$\nabla \cdot (\sigma \mathbf{E}) = 0. \tag{5}$$

In this equation $\sigma = (z_+ \mu_+ c_+ + z_- \mu_- c_-)F \simeq z_+ c_+ (\mu_+ - \mu_-)F$ denotes the electrical conductivity of the symmetric binary electrolyte. To model the transport of electrical conductivity, we multiply the transport equation for the cation, Eq. (4) with $z_+(\mu_+ - \mu_-)F$ and eliminate $\mathbf{E}$ using Eq. (5) to get

$$\frac{\partial \sigma}{\partial t} + \mathbf{u} \cdot \nabla \sigma = D_0 \nabla^2 \sigma. \tag{6}$$

Lastly, we note that for low current density and displacement current $\partial(\epsilon \mathbf{E})/\partial t$, electric field can be assumed to be quasistatic. Hence, from Maxwell's equations

$$\nabla \times \mathbf{E} = \mathbf{0}. \tag{7}$$

To simplify our analysis we can therefore introduce an electric potential ϕ, which is related to the electric field by $\mathbf{E} = -\nabla\phi$.

Equations (2)–(3), (5), and (6)–(7) describe EHD flow in a symmetric binary electrolyte due to diffusive conductivity gradients. We note that, while deriving the governing equations, we have assumed electroneutrality for mass conservation of ionic species but included a body force due to free

charge in the momentum conservation equation, Eq. (3). The electroneutrality assumption is valid for mass conservation because the difference in the concentrations of cations and anions is very small compared with the bulk concentration of ions. However, the free charge due to this small difference in cation and anion concentrations is significant enough to cause an appreciable body force on the fluid [15–17].

B. Dimensionless governing equations

We choose the following scales for non-dimensionalizing the governing equations:

$$[x,y,z] = d, \quad [\mathbf{E}] = E_a, \quad [\mathbf{u}] = U_{ev}, \quad [t] = \frac{d}{U_{ev}},$$
$$[p] = \epsilon E_a^2, \quad [\sigma] = \sigma_a, \tag{8}$$

where σ_a and E_a denote the local conductivity and electric field at the lower boundary ($z = 0$), respectively. The appropriate reference scale for velocity is the electroviscous velocity, $U_{ev} = \epsilon E_a^2 d/\eta$, which is obtained by balancing the electric body force and viscous stresses.

Non-dimensionalizing the governing equations, Eqs. (2)–(3), (5), and (6)–(7), using these references scales, we obtain

$$\nabla \cdot \mathbf{u} = 0, \tag{9}$$

$$\frac{\tau_v}{\tau_{ev}}\left(\frac{\partial \mathbf{u}}{\partial t} + \mathbf{u}\cdot\nabla\mathbf{u}\right) = -\nabla p + \nabla^2\mathbf{u} + (\nabla\cdot\mathbf{E})\mathbf{E} \tag{10}$$

$$\nabla \times \mathbf{E} = \mathbf{0}, \tag{11}$$

$$\nabla \cdot (\sigma\mathbf{E}) = 0, \tag{12}$$

$$\frac{D\sigma}{Dt} = \frac{1}{\mathrm{Ra}_e}\nabla^2\sigma. \tag{13}$$

Here $\tau_{ev} = \eta/(\epsilon E_a^2)$ and $\tau_v = \rho d^2/\eta$ are the time scales associated with electroviscous flow and momentum diffusion, respectively. Whereas the dimensionless parameter Ra_e is the electric Rayleigh number given by $\mathrm{Ra}_e = \epsilon E_a^2 d^2/(\eta D_0)$. The electric Rayleigh number is the ratio of time scale associated with diffusion of conductivity ($\tau_d = d^2/D_0$) and the electroviscous time scale τ_{ev}. Based on the dimensionless governing equations, Eqs. (9)–(13), we now analyze the linear stability of EHD flow.

C. Linear stability analysis

In the quiescent base state, the dimensionless velocity, electric field, and pressure distribution are given by

$$\bar{\mathbf{u}} = 0, \quad \bar{\mathbf{E}} = \frac{1}{\bar{\sigma}}\mathbf{e_z}, \quad \bar{p} = \frac{\bar{E}(z)^2}{2}. \tag{14}$$

To analyze the linear stability of the system in this base state, we introduce the following perturbation variables (with primes):

$$\mathbf{u} = \mathbf{u}', \quad p = \bar{p} + p',$$
$$\mathbf{E} = \bar{\mathbf{E}} + \mathbf{E}', \quad \sigma = \bar{\sigma} + \sigma'. \tag{15}$$

Substituting these variables in the dimensionless governing equations, Eqs. (9)–(13), and neglecting the higher order terms in perturbation variables, we obtain the following linearized governing equations:

$$\nabla \cdot \mathbf{u}' = 0, \tag{16}$$

$$\frac{\tau_v}{\tau_{ev}}\frac{\partial \mathbf{u}'}{\partial t} = -\nabla p' + \nabla^2\mathbf{u}' + \bar{\mathbf{E}}\nabla\cdot\mathbf{E}' + \mathbf{E}'\nabla\cdot\bar{\mathbf{E}}, \tag{17}$$

$$\nabla\cdot(\sigma'\bar{\mathbf{E}}) + \nabla\cdot(\bar{\sigma}\mathbf{E}') = 0, \tag{18}$$

$$\frac{\partial\sigma'}{\partial t} + \mathbf{u}'\cdot\nabla\bar{\sigma} = \frac{1}{\mathrm{Ra}_e}\nabla^2\sigma', \tag{19}$$

$$\nabla\times\mathbf{E}' = \mathbf{0}. \tag{20}$$

Noting that the electric field is irrotational, we can simplify Eqs. (17) and (18) by introducing electric potentials $\bar{\phi}$ and ϕ' corresponding to the base state and the perturbed state, respectively, to get

$$\frac{\tau_v}{\tau_{ev}}\frac{\partial \mathbf{u}'}{\partial t} = -\nabla p' + \nabla^2\mathbf{u}' + \frac{d\bar{\phi}}{dz}\mathbf{e}_z\nabla^2\phi' + \frac{d^2\bar{\phi}}{dz^2}\nabla\phi', \tag{21}$$

$$\frac{d}{dz}\left(\sigma'\frac{d\bar{\phi}}{dz}\right) + \nabla\cdot(\bar{\sigma}\nabla\phi') = 0. \tag{22}$$

Here, $\mathbf{e}_z$ denotes the unit vector pointing in the positive z-direction. Next, to eliminate pressure and x and y components of velocity, we take the curl of Eq. (21) twice and then use the continuity equation, Eq. (16), to get

$$\left(\frac{\tau_v}{\tau_{ev}}\frac{\partial}{\partial t} - \nabla^2\right)\nabla^2 w' = \frac{d\bar{\phi}}{dz}\left(\nabla^2\nabla_1^2\phi'\right) - \frac{d^3\bar{\phi}}{dz^3}\nabla_1^2\phi',$$

where

$$\nabla_1^2 \equiv \frac{\partial^2}{\partial x^2} + \frac{\partial^2}{\partial y^2}. \tag{23}$$

Equations (19), (22), and (23) form a coupled set of equations in terms of perturbation variables: electric potential ϕ', conductivity σ', and z-component of the flow velocity, w'. To solve these equations, we require four boundary conditions at each boundary $z = 0$ and $z = 1$. First, we assume that the perturbations in velocity and electric field vanish at the boundaries. We also assume that the perturbation in conductivity vanishes at the boundaries, as the boundaries are maintained at a constant conductivity. These boundary conditions can be expressed as

$$w' = 0, \quad \sigma' = 0, \quad \frac{\partial\phi'}{\partial z} = 0 \text{ at } z = 0,1. \tag{24}$$

The remaining boundary conditions can be obtained depending on whether the boundaries are stress-free or rigid [18],

$$\frac{\partial^2 w'}{\partial z^2} = 0 \text{ (stress-free) or } \frac{\partial w'}{\partial z} = 0 \text{ (rigid) at } z=0,1. \tag{25}$$

D. Normal mode analysis

Since the governing equations (19), (22), (23) and boundary conditions (24) and (25) are linear, we can analyze the stability of the overall system by considering stability of individual perturbations using the normal mode analysis. We assume the

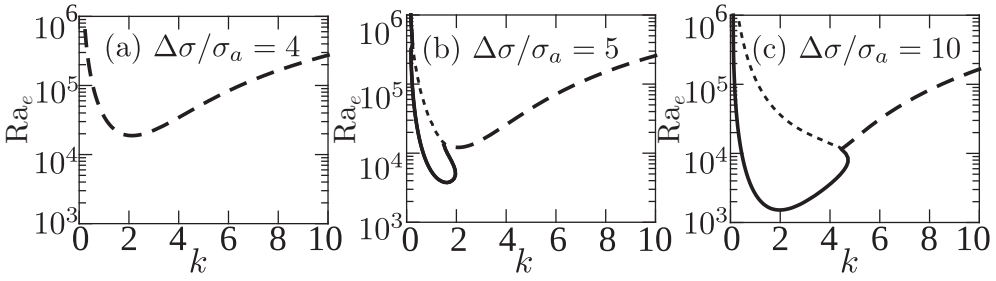

FIG. 2. Neutral stability curves for (a) $\Delta\sigma/\sigma_a = 4$, (b) $\Delta\sigma/\sigma_a = 5$, and (c) $\Delta\sigma/\sigma_a = 10$ with stress-free boundaries. Solid lines: least stable stationary mode; dashed lines: least stable oscillatory mode; dotted line: second least stable stationary mode. At low conductivity gradients, the least stable mode is oscillatory. At higher conductivity gradients, stationary and oscillatory modes dominate at low and high wave numbers, respectively.

following form for perturbation variables:

$$\phi' = \hat{\phi}(z)e^{st+ik_x x+ik_y y}, \quad w' = \hat{w}(z)e^{st+ik_x x+ik_y y},$$
$$\sigma' = \hat{\sigma}(z)e^{st+ik_x x+ik_y y}. \tag{26}$$

Here, s and k denote dimensionless growth rate and wave number of perturbation, respectively. In general, the growth rate is complex valued, that is, $s = \mathrm{Re}(s) + i\mathrm{Im}(s)$. Substituting this form of solution for perturbation variables in Eqs. (19), (22), and (23) we obtain the following coupled ordinary differential equations in $\hat{w}$, $\hat{\phi}$, and $\hat{\sigma}$:

$$\left(\frac{\tau_v}{\tau_{ev}}s - (D^2-k^2)\right)(D^2-k^2)\hat{w} = k^2\left(\frac{d^3\overline{\phi}}{dz^3} - \frac{d\overline{\phi}}{dz}(D^2-k^2)\right)\hat{\phi}, \tag{27}$$

$$\left(\overline{\sigma}(D^2-k^2) + \frac{d\overline{\sigma}}{dz}D\right)\hat{\phi} + \left(\frac{d^2\overline{\phi}}{dz^2} + \frac{d\overline{\phi}}{dz}D\right)\hat{\sigma} = 0, \tag{28}$$

$$s\hat{\sigma} + \hat{w}\frac{d\overline{\sigma}}{dz} = \frac{1}{\mathrm{Ra}_e}(D^2-k^2)\hat{\sigma}, \tag{29}$$

where $D \equiv d/dz$ and $k^2 = k_x^2 + k_y^2$. Equations (27)–(29) can be solved using the boundary conditions given by Eqs. (24) and (25). For normal mode analysis, these boundary conditions simplify to

$$\hat{w} = 0, \quad D^2\hat{w} = 0, \quad \hat{\sigma} = 0, \quad D\hat{\phi} = 0 \text{ at } z = 0,1. \tag{30}$$

for stress-free boundaries and

$$\hat{w} = 0, \quad D\hat{w} = 0, \quad \hat{\sigma} = 0, \quad D\hat{\phi} = 0 \text{ at } z = 0,1 \tag{31}$$

for rigid boundaries.

III. RESULTS AND DISCUSSION

Equations (27)–(29) along with boundary conditions, Eqs. (30) and (31), define an eigenvalue problem with growth rates s as the eigenvalues and functions $\hat{w}$, $\hat{\phi}$, and $\hat{\sigma}$ as the corresponding eigenmodes. We solve this eigenvalue problem using a pseudospectral collocation method with Chebyshev polynomials as the basis functions [19]. For all our calculations, we consider parameters that are typical of electrophoresis techniques in aqueous medium: $\eta = 1 \times 10^{-3}$ Pa s, $\rho = 1000$ kg m^{-3}, $\epsilon = 7.08 \times 10^{-10}$ F m^{-1}, $D_0 = 10^{-9}$ m^2 s^{-1}.

A. Stability characteristics for stress-free boundaries

In Figs. 2(a)–2(c) we present neutral stability curves (Ra_e versus k) for conductivity ratios of $\Delta\sigma/\sigma_a = 4$, 5, and 10, respectively, for stress-free boundaries. The neutral stability curves correspond to those values of Ra_e and k for which the real part of growth rate s for least stable eigenmode is zero. In Fig. 2, the solid and dashed neutral stability curves correspond to eigenmodes which are stationary [$\mathrm{Im}(s) = 0$] and oscillatory [$\mathrm{Im}(s) \neq 0$], respectively. In addition to the least stable mode, in Figs. 2(b) and 2(c) we also show the neutral stability curves for the second least stable stationary mode with dotted lines. Note that, oscillatory modes corresponding to leading two eigenvalues occur in pairs, and have complex conjugate growth rates with equal $\mathrm{Re}(s)$. The neutral stability curves in Fig. 2 compare well with the predictions of Chang *et al.* [13]. At $\Delta\sigma/\sigma_a = 4$ the system shows overstability as evidenced by complex valued growth rates. At high conductivity ratios of $\Delta\sigma/\sigma_a = 5$ and 10, the stationary and oscillatory modes dominate at low and high wave numbers, respectively.

The EHD instability is driven by the electric body force which results due to the coupling of local electric field and free charge in the bulk solution. As described by Eq. (17), the perturbation in electric body force due to small disturbances in the conductivity field has two contributions, $\overline{\mathbf{E}}\nabla\cdot\mathbf{E}'$ and $\mathbf{E}'\nabla\cdot\overline{\mathbf{E}}$. The effect of these forces can be visualized by considering a low conductivity fluid parcel which is displaced to a high conductivity region. The change in local conductivity of the fluid due to this disturbance induces a perturbation charge $\nabla\cdot\mathbf{E}'$, which couples with the base-state electric field, $\overline{\mathbf{E}}$, to apply a body force $\overline{\mathbf{E}}\nabla\cdot\mathbf{E}'$ on the fluid. The disturbance in local conductivity also alters the local electric field, $\mathbf{E}'$, which couples with the free charge in the base state $\nabla\cdot\overline{\mathbf{E}}$ to apply a body force $\mathbf{E}'\nabla\cdot\overline{\mathbf{E}}$ on the fluid. Both of these forces are Coulombic in nature. The $\overline{\mathbf{E}}\nabla\cdot\mathbf{E}'$ and $\mathbf{E}'\nabla\cdot\overline{\mathbf{E}}$ forces correspond to the terms $-k^2 d\overline{\phi}/dz(D^2-k^2)\hat{\phi}$ and $k^2 d^3\overline{\phi}/dz^3\hat{\phi}$ in Eq. (27), respectively.

To estimate the conditions at which the $\overline{\mathbf{E}}\nabla\cdot\mathbf{E}'$ and $\mathbf{E}'\nabla\cdot\overline{\mathbf{E}}$ forces dominate, we consider a general perturbation $\hat{\phi} \propto \cos(m\pi z)$, were m is an integer. The ratio of these forces in Eq. (27) evaluated at lower boundary, where electric body forces are highest due to high local electric field, is given by

$$\left.\frac{-d\overline{\phi}/dz(D^2-k^2)\hat{\phi}}{d^3\overline{\phi}/dz^3\hat{\phi}}\right|_{z=0} = \frac{((m\pi)^2+k^2)}{2(\Delta\sigma/\sigma_a)^2}. \tag{32}$$

This equation shows that the $\overline{\mathbf{E}}\nabla\cdot\mathbf{E}'$ force dominates when conductivity ratio $\Delta\sigma/\sigma_a$ is low or wave number k is high. Whereas, $\mathbf{E}'\nabla\cdot\overline{\mathbf{E}}$ force dominates for high conductivity ratios and low wave number disturbances. The neutral stability curves presented in Fig. 2 therefore suggest that the EHD instability is characterized by oscillatory and stationary modes when $\overline{\mathbf{E}}\nabla\cdot\mathbf{E}'$ force and $\mathbf{E}'\nabla\cdot\overline{\mathbf{E}}$ force dominate, respectively. To validate this hypothesis, we consider two limiting cases of vanishingly low and very high base-state conductivity gradients where either one of these forces dominate.

B. Limit of low base-state conductivity gradient

In the limit of vanishingly small base-state conductivity gradient $\Delta\sigma/\sigma_a \ll 1$, we can perform regular asymptotic analysis of the governing equations, Eqs. (27)–(29), taking $\alpha = \Delta\sigma/\sigma_a$ as the small parameter. We expand $\hat{w}$, $\hat{\phi}$, $\hat{\sigma}$, and s as follows:

$$\hat{w} = \hat{w}_0 + \alpha\hat{w}_1 + O(\alpha^2), \quad \hat{\phi} = \hat{\phi}_0 + \alpha\hat{\phi}_1 + O(\alpha^2),$$
$$\hat{\sigma} = \hat{\sigma}_0 + \alpha\hat{\sigma}_1 + O(\alpha^2), \quad s = s_0 + \alpha s_1 + O(\alpha^2). \tag{33}$$

Substituting this form of variables in Eqs. (27)–(29) and evaluating base-state quantities in the limit of $\alpha = \Delta\sigma/\sigma_a \ll 1$ yields the following leading order approximation of the governing equations:

$$\left(\frac{\tau_v}{\tau_{ev}}s_0 - (D^2-k^2)\right)(D^2-k^2)\hat{w}_0 = k^2(D^2-k^2)\hat{\phi}_0, \tag{34}$$

$$(D^2-k^2)\hat{\phi}_0 = D\hat{\sigma}_0, \tag{35}$$

$$s_0\hat{\sigma}_0 + \hat{w}_0\frac{\Delta\sigma}{\sigma_a} = \frac{1}{\mathrm{Ra}_e}(D^2-k^2)\hat{\sigma}_0. \tag{36}$$

An approximate way of deriving these equations is to evaluate the base-state quantities in Eqs. (27)–(29) and set $\Delta\sigma/\sigma_a = 0$, except in Eq. (29) because $\mathrm{Ra}_e\Delta\sigma/\sigma_a$ is not small. Interestingly, in the limit of $\alpha = \Delta\sigma/\sigma_a \ll 1$ only the $\overline{\mathbf{E}}\nabla\cdot\mathbf{E}'$ force is present [see right hand side of Eq. (34)]. The other force $\mathbf{E}'\nabla\cdot\overline{\mathbf{E}}$ (or $k^2d^3\overline{\phi}/dz^3\hat{\phi}$) in Eq. (27) appears at the higher order $O(\alpha^2)$ which implies that it is not responsible for EHD instability when the base-state conductivity gradient is small.

In Fig. 3(a), we present the neutral stability curves for $\Delta\sigma/\sigma_a = 0.05$ computed using the exact governing equations, Eqs. (27)–(29), and the approximate equations, Eqs. (34)–(36), for low conductivity gradient. For $\Delta\sigma/\sigma_a = 0.05$, the least stable mode for all wave numbers is oscillatory in nature; Fig. 3(b) shows imaginary part of growth rate $\mathrm{Im}(s)$ versus k for neutrally stable modes. The neutral stability curves and the imaginary part of growth rate obtained using the approximate equations for $\Delta\sigma/\sigma_a \ll 1$ closely match those predicted using the exact set of governing equations. This validates our hypothesis that only $\overline{\mathbf{E}}\nabla\cdot\mathbf{E}'$ force is responsible for EHD instability at low conductivity gradients.

To elucidate the physical mechanism governing the overstability at low conductivity gradients, in Figs. 3(c) and 3(d) we plot the eigenmodes, p', σ', $\mathbf{E}'$, and streamlines for $\mathbf{u}'$, corresponding to the critical state for $\Delta\sigma/\sigma_a = 0.05$, ($k = 3$, $\mathrm{Ra}_e = 8.3\times10^5$). The eigenmodes for conductivity and convection cells patterns are inclined and indicate a traveling wave propagating horizontally towards the left, as

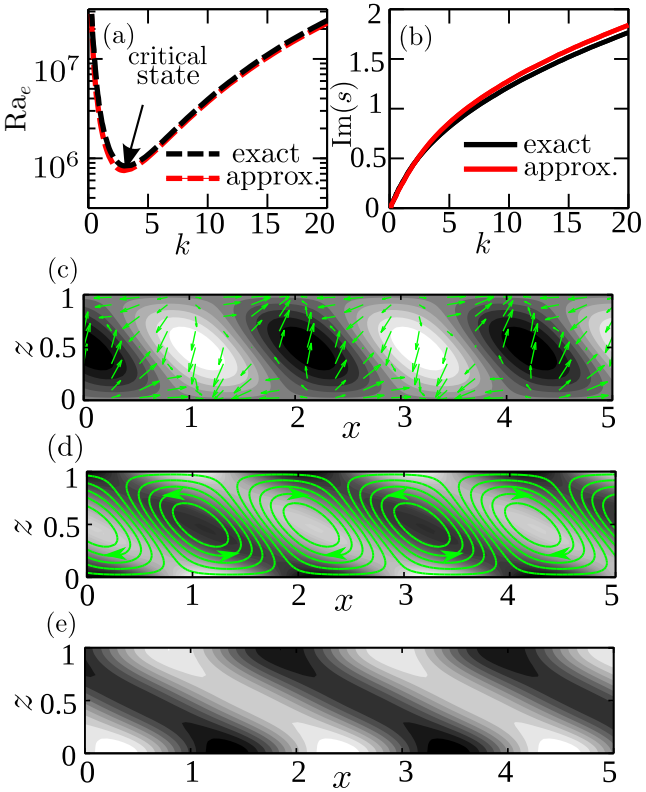

FIG. 3. (a) Neutral stability curves, Ra_e versus k, for $\Delta\sigma/\sigma_a = 0.05$. (b) $\mathrm{Im}(s)$ versus wave number k. (c)–(e) Eigenmodes corresponding to the critical state ($k = 3$, $\mathrm{Ra}_e = 8.3\times10^5$). Dark gray is negative and light gray is positive. (c) Perturbation conductivity σ' and electric field $\mathbf{E}'$ (arrows). (d) Convection cell patterns (streamlines) for $\mathbf{u}'$ and perturbation pressure p'. (e) Spatial variation of perturbation charge $\nabla\cdot\mathbf{E}'$.

$\mathrm{Im}(s) > 0$. Because this instability is driven only by $\overline{\mathbf{E}}\nabla\cdot\mathbf{E}'$ force, in Fig. 3(e) we show the perturbation charge $\nabla\cdot\mathbf{E}'$ resulting from the perturbation in conductivity field. The perturbation charge accumulates along the inclined interfaces of the perturbation conductivity modes. The inclined interfaces bounded by high (low) conductivity on the left and low (high) conductivity on the right acquire a positive (negative) charge. The perturbation charge couples with the base-state electric field to apply a $\overline{\mathbf{E}}\nabla\cdot\mathbf{E}'$ force in the tangential direction of the conductivity modes. This tangential force drives inclined cellular motion which draws high conductivity fluid from top and low conductivity fluid from bottom. Consequently, the instability modes propagate towards the left, which is consistent with $\mathrm{Im}(s) > 0$. We note that similar mechanism was proposed by Hoburg and Melcher [10] although they did not attribute oscillatory modes primarily to $\overline{\mathbf{E}}\nabla\cdot\mathbf{E}'$ force.

C. Limit of large base-state conductivity gradient

Next, we consider the opposite case of very high conductivity ratio $\Delta\sigma/\sigma_a = 50$. The neutral stability curve for this case [Fig. 4(a)] qualitatively resembles that for $\Delta\sigma/\sigma_a = 10$ shown in Fig. 2(c). To check whether the $\mathbf{E}'\nabla\cdot\overline{\mathbf{E}}$ force dominates at high conductivity gradients, we artificially exclude the term $-k^2d\overline{\phi}/dz(D^2-k^2)\hat{\phi}$ corresponding to $\overline{\mathbf{E}}\nabla\cdot\mathbf{E}'$ force in Eq. (27) and compute the neutral stability curves. As shown

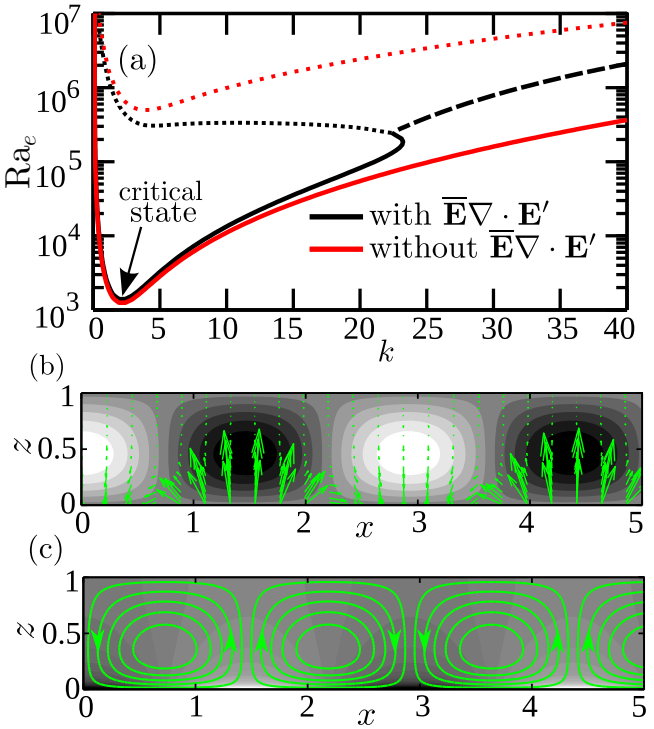

FIG. 4. (a) Neutral stability curves, Ra_e versus k, for $\Delta\sigma/\sigma_a = 50$, with and without $\overline{\mathbf{E}}\nabla\cdot\mathbf{E}'$ force. (b),(c) Eigenmodes corresponding to the critical state ($k = 2.16$, $\mathrm{Ra}_e = 1376$). Dark gray is negative and light gray is positive. (b) Perturbation conductivity σ' and electric field $\mathbf{E}'$ (arrows). (c) Convection cell patterns (streamlines) for $\mathbf{u}'$ and perturbation pressure p'.

in Fig. 4(a) the neutral stability curves for cases with and without $\overline{\mathbf{E}}\nabla\cdot\mathbf{E}'$ force agree well, particularly at low wave numbers where the $\mathbf{E}'\nabla\cdot\overline{\mathbf{E}}$ force dominates. This provides a conclusive evidence that the EHD instability with stationary mode results due to the $\mathbf{E}'\nabla\cdot\overline{\mathbf{E}}$ force. We note that, Hoburg and Melcher [10] predicted stationary modes at low wave numbers even in the absence of diffusion. Therefore, contrary to the mechanism proposed by Chang *et al.* [13], diffusion cannot be the cause for existence of stationary modes. The diffusion of conductivity has a stabilizing effect on the flow and it leads to a threshold value of electric Rayleigh number above which the instability sets in. Interestingly, for the case where $\overline{\mathbf{E}}\nabla\cdot\mathbf{E}'$ force is neglected, in Fig. 4(a) we observe that oscillatory mode is absent at high wave numbers. This corroborates with our conclusion that the $\overline{\mathbf{E}}\nabla\cdot\mathbf{E}'$ force is responsible for overstability.

It remains to describe the physical mechanism of how $\mathbf{E}'\nabla\cdot\overline{\mathbf{E}}$ force destabilizes the system through a stationary mode. To this end, in Figs. 4(b) and 4(c) we present the eigenmodes p', σ', $\mathbf{E}'$, and streamlines for $\mathbf{u}'$ corresponding to the critical state for $\Delta\sigma/\sigma_a = 50$, ($k = 2.16$, $\mathrm{Ra}_e = 1376$). The critical mode is characterized by stationary cellular convection which results from the $\mathbf{E}'\nabla\cdot\overline{\mathbf{E}}$ force. This is because, in the base state, a positive gradient in conductivity and a negative gradient in electric field results in negative free charge ($\nabla\cdot\overline{\mathbf{E}}$) in the bulk liquid. To balance the base-state electric body force, the pressure near the lower boundary is higher than that near the upper boundary. When a parcel of low-conductivity fluid is displaced upwards, due to the Ohm's law, Eq. (12), the local electric field increases in the region where the low-conductivity fluid displaces the high-conductivity fluid [see Fig. 4(b)]. The additional body force due to the coupling of base-state free charge and perturbation electric field $\mathbf{E}'\nabla\cdot\overline{\mathbf{E}}$ acts downwards along the direction of base-state electric body force $\overline{\mathbf{E}}\nabla\cdot\overline{\mathbf{E}}$. Consequently, the pressure gradient increases in the region where low conductivity fluid displaces high conductivity fluid, and this drives an upward destabilizing flow. Similarly, when a fluid parcel with higher-conductivity is displaced downwards, it drives a downward destabilizing flow. As a result, stationary convection cells form [Fig. 4(c)] which further amplify the conductivity disturbance.

D. Rigid boundaries

The physical mechanism proposed above for switching between stationary and oscillatory modes of EHD instability is independent of whether the fluid layer is bounded by stress-free or rigid boundaries. This is because our analysis is based on comparing the relative magnitudes of $\overline{\mathbf{E}}\nabla\cdot\mathbf{E}'$ and $\mathbf{E}'\nabla\cdot\overline{\mathbf{E}}$ forces in the momentum equation, Eq. (17), and not the boundary conditions, Eq. (31). To demonstrate this, in Figs. 5(a) and 5(b), we present the neutral stability curves and the imaginary part of growth rate, respectively, for $\Delta\sigma/\sigma_a = 0.05$ computed for rigid boundary conditions, Eq. (31). Similar to the results presented in Fig. 3 for stress-free boundaries, the neutral stability curves and the imaginary part of growth rate obtained for rigid boundaries using the exact governing equations (27)–(29) and the approximate equations (34)–(36) for low conductivity gradient match closely. Because only the $\overline{\mathbf{E}}\nabla\cdot\mathbf{E}'$ force is present in Eqs. (34)–(36) for low conductivity gradient limit, we conclude that even for rigid boundaries, only $\overline{\mathbf{E}}\nabla\cdot\mathbf{E}'$ force is responsible for overstability at low conductivity gradients.

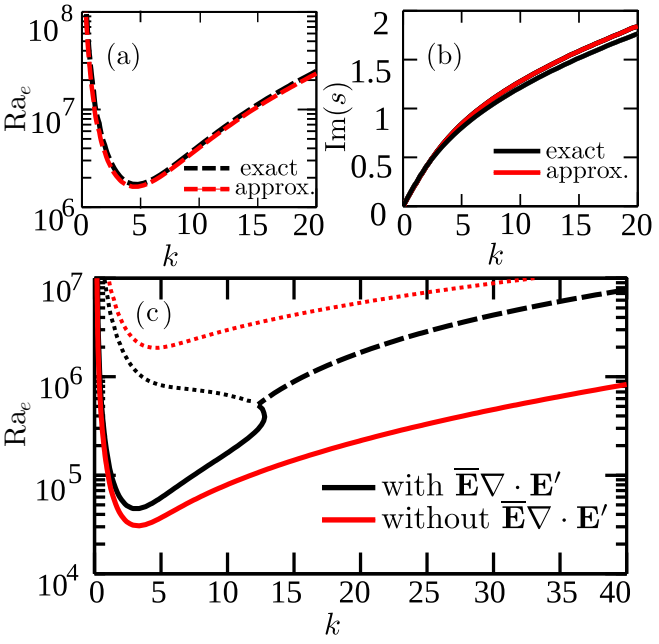

FIG. 5. Stability characteristics for rigid boundaries. (a) Neutral stability curves, Ra_e versus k, for $\Delta\sigma/\sigma_a = 0.05$. (b) Im($s$) versus wave number k. (c) Neutral stability curves, Ra_e versus k, for $\Delta\sigma/\sigma_a = 100$, with and without the $\overline{\mathbf{E}}\nabla\cdot\mathbf{E}'$ force.

Next, in Fig. 5(c) we present the neutral stability curves for a large conductivity gradient of $\Delta\sigma/\sigma_a = 100$ with rigid boundaries. Similar to Fig. 4(a) for stress-free boundaries, in Fig. 5(c) we present results for exact governing equations and by excluding the $\overline{\mathbf{E}}\nabla\cdot\mathbf{E}'$ term. The neutral stability curves for cases with and without $\overline{\mathbf{E}}\nabla\cdot\mathbf{E}'$ force agree well at low wave numbers where the $\mathbf{E}'\nabla\cdot\overline{\mathbf{E}}$ force dominates. Moreover, the oscillatory mode is absent at high wave numbers when the $\overline{\mathbf{E}}\nabla\cdot\mathbf{E}'$ term is neglected. Therefore, we conclude that even for rigid boundaries, the body force due to the coupling of base-state electric field and perturbation charge is responsible for overstability. Whereas, the body force due to the coupling of base-state charge and perturbation electric field leads to stationary modes of instability. We note that quantitative differences between the results for stress-free and rigid boundaries exist because the rigid boundaries have a stabilizing effect on the flow [13].

IV. CONCLUDING REMARKS

We have shown that the electric body force which is responsible for EHD instability with collinear conductivity gradient and electric field can be considered as a combination of $\overline{\mathbf{E}}\nabla\cdot\mathbf{E}'$ and $\mathbf{E}'\nabla\cdot\overline{\mathbf{E}}$ forces. The $\overline{\mathbf{E}}\nabla\cdot\mathbf{E}'$ force which results from the coupling of perturbation free charge and base-state electric field leads to overstability. Whereas, the $\mathbf{E}'\nabla\cdot\overline{\mathbf{E}}$ force resulting for the coupling of perturbation electric field with base-state free charge leads to EHD instability via a stationary mode. This mechanism correctly explains the existence of oscillatory modes at low conductivity gradients and high wave number disturbances where the $\overline{\mathbf{E}}\nabla\cdot\mathbf{E}'$ force dominates. Whereas, for low wave number disturbances for which the $\mathbf{E}'\nabla\cdot\overline{\mathbf{E}}$ force dominates, the physical mechanism correctly identifies stationary cellular convection as the mode of EHD instability. Contrary to the mechanism proposed earlier by Chang *et al.* [13], we have shown that the selection of stationary and oscillatory modes does not depend on molecular diffusion.

ACKNOWLEDGMENT

We acknowledge the financial support received from the Science and Engineering Research Board (SERB), Government of India under Grant No. SERB/F/2665/2014-2015.

[1] K. Seiler, Z. H. Fan, K. Fluri, and D. J. Harrison, Anal. Chem. **66**, 3485 (1994).
[2] S. S. Bahga, O. I. Vinogradova, and M. Z. Bazant, J. Fluid Mech. **644**, 245 (2010).
[3] R. Bharadwaj and J. G. Santiago, J. Fluid Mech. **543**, 57 (2005).
[4] B. Bjellqvist, K. Ek, P. G. Righetti, E. Gianazza, A. Görg, R. Westermeier, and W. Postel, J. Biochem. Bioph. Meth. **6**, 317 (1982).
[5] S. S. Bahga and J. G. Santiago, Analyst **138**, 735 (2013).
[6] B. Jung, R. Bharadwaj, and J. G. Santiago, Electrophoresis **24**, 3476 (2003).
[7] A. E. Herr, J. I. Molho, K. A. Drouvalakis, J. C. Mikkelsen, P. J. Utz, J. G. Santiago, and T. W. Kenny, Anal. Chem. **75**, 1180 (2003).
[8] H. Lin, Mech. Res. Commun. **36**, 33 (2009).
[9] J. R. Melcher, *Continuum Electromechanics* (MIT Press, Cambridge, MA, 1981).
[10] J. F. Hoburg and J. R. Melcher, Phys. Fluids **20**, 903 (1977).
[11] J. C. Baygents and F. Baldessari, Phys. Fluids **10**, 301 (1998).
[12] A. O. El Moctar, N. Aubry, and J. Batton, Lab Chip **3**, 273 (2003).
[13] M. H. Chang, A. C. Ruo, and F. Chen, J. Fluid Mech. **634**, 191 (2009).
[14] A. Castellanos, A. Ramos, A. Gonzalez, N. G. Green, and H. Morgan, J. Phys. D Appl. Phys. **36**, 2584 (2003).
[15] V. G. Levich, *Physicochemical Hydrodynamics*, 2nd ed. (Prentice-Hall, Englewood Cliffs, NJ, 1962).
[16] C.-H. Chen, H. Lin, S. K. Lele, and J. G. Santiago, J. Fluid. Mech. **524**, 263 (2005).
[17] A. Ramos, *Electrokinetics and Electrohydrodynamics in Microsystems* (Springer, New York, 2011).
[18] S. Chandrasekhar, *Hydrodynamic and Hydromagnetic Stability* (Dover Publications, New York, 1981).
[19] J. P. Boyd, *Chebyshev and Fourier Spectral Methods* (Dover, New York, 2001).